

7. Zhang Ch. A 2D hypersingular time-domain traction BEM for transient elastodynamic crack analysis. *Wave Motion*. 2002. Vol. 35. No. 1. P. 17–40. [https://doi.org/10.1016/S0165-2125\(01\)00081-6](https://doi.org/10.1016/S0165-2125(01)00081-6)
8. Поручиков В. Б. Методы динамической теории упругости. М.: Наука, 1986. 328 с.
9. Попов В. Г. Сравнение полей перемещений и напряжений при дифракции упругих волн сдвига на различных дефектах: трещина и тонкое жесткое включение. *Динам. системы*. 1993. Вып. 12. С. 35–41.
10. Векуа И. Н. Новые методы решения эллиптических уравнений. М.: ОГИЗ, 1948. 296 с.
11. Белоцерковский С. М., Лифанов И. К. Численные методы в сингулярных интегральных уравнениях. М.: Наука, 1985. 253 с.
12. Кирилова О. І., Михаськів В. В. Плоска динамічна задача для циліндричного тіла довільного перерізу з тонким жорстким включенням. *Вісн. Київ. нац. ун-ту. Сер. Фіз.-мат. науки*. 2015. № 5. С. 167–173.
13. Кирилова О. І., Попов В. Г. Напружений стан у нескінченному циліндрі довільного перерізу з тунельною тріщиною при коливаннях в умовах плоскої деформації. *Вісн. Київ. нац. ун-ту. Сер. Фіз.-мат. науки*. 2017. № 3. С. 71–74.

DOI: <https://doi.org/10.15407/pmach2019.01.024>

UDC 539.3

MAJOR STRESS-STRAIN STATE OF DOUBLE SUPPORT MULTILAYER BEAMS UNDER CONCENTRATED LOAD

Part 2. Model Implementation and Calculation Results

Stanislav B. Kovalchuk
stanislav.kovalchuk@pdaa.edu.ua
 ORCID: 0000-0003-4550-431X

Oleksii V. Goryk
 ORCID: 0000-0002-2804-5580

Poltava State Agrarian Academy
 1/3, Skovorody St., Poltava,
 36003, Ukraine

The development of composite technologies contributes to their wide introduction into the practice of designing modern different-purpose structures. Reliable prediction of the stress-strain state of composite elements is one of the conditions for creating reliable structures with optimal parameters. Analytical theories for determining the stress-strain state of multilayer rods (bars, beams) are significantly inferior in development to those for composite plates and shells, although their core structural elements are most common. The purpose of this paper is to design an analytical model for bending double support multilayer beams under a concentrated load, with the model based on the previously obtained elasticity theory solution for a multi-layer cantilever. The second part of the article contains examples of the implementation of the model for bending double-support multi-layer beams under a concentrated load, with the model constructed in the first part of the article. Using this model, solutions to the problems of bending multilayer beams with different types of fixation of their extreme cross-sections were obtained. The resultant relations were approximated using test problems for determining the deflections of homogeneous composite double-support beams with different combinations of fixation, as well as in determining the stresses and displacements of a four-layer beam with a combination of a rigid and hinged fixation at its ends. The results obtained have a slight discrepancy with the simulation results by the finite element method (FEM) and the calculation by the iterative model for bending composite bars, even for relatively short beams. In addition, it is shown that the neglect of the shear amenability of layer materials results in large errors in determining the deflections, and in the case of statically indefinable beams, reactive forces and stresses. The approach used in the construction of the model can be extended to the case of beams with arbitrary numbers of concentrated forces and intermediate supports, and to calculate multilayer beams with different rigidity of their design sections.

Keywords: multilayer beam, orthotropic layer, concentrated load, deflection, stresses, displacements.

Introduction

The mechanics of deformation of composite multilayer plates and shells is the subject of a large number of fundamental scientific works [1–8]. The deformation of composite rods (bars, beams) is less studied, although such structural elements are most common.

When a problem of bending composite beams is solved, there is a wide spread use of refined models, in particular, constructed by an iterative method [9–11]. Such models are quite universal, however, they are very cumbersome and difficult for practical use at high refinement steps. At the same time, exact solutions for multi-layer beams, for example [12, 13], are limited in the capability of taking into account different types of

© Stanislav B. Kovalchuk, Oleksii V. Goryk, 2019

loads and supports. However, on their basis, we can obtain relatively simple, but fairly accurate applied solutions to typical problems.

In the first part of paper [14], we constructed an analytical simple bending model of a two-support multi-layer beam under a concentrated load. To construct it, we used a general solution of the theory of elasticity for a multi-layer cantilever beam with a load at the end [12]. The purpose of this part of the paper is to demonstrate the application of the constructed model to the most common schemes for fixing two-support beams under a concentrated load, as well as approximating the relations obtained in the process of solving test problems.

Main part

The simple bending model of a two-support multilayer beam under a concentrated load, built in the first part of article [14], comprises: relations (2)–(4) for the components of the main SSS of beam segments, system of equations (10) for determining the initial parameters of a beam, as well as the dependencies between the initial parameters of the first and second sections (11). The relations for the SSS components contain 6 static (values of internal force factors $N_{x1}^{(i)}, Q_{z1}^{(i)}, M_{y1}^{(i)}, i=1,2$) and 6 kinematic (displacement values $u_{11}^{(i)}, u_{12}^{(i)}, w_{11}^{(i)}, i=1,2$) initial parameters, which depend on the type of beam fixation at the ends. In each specific case of fixation, 6 out of 12 parameters can be specified directly, and the remaining 6 can be determined by solving the system of algebraic equations (10) [14].

Consider the main stages of the implementation of the model in determining the basic SSS of hinged end, fixed end, and fixed-hinged beams.

Hinged End Beams. Let us assume that the left hinge support of the beam is fixed, and the right one does not limit the longitudinal movement of the fixed point (Fig. 1).

For this method of fixing the ends of a beam, we can directly specify the following static and kinematic conditions for the initial and final cross-sections:

$$M_{y1}^{(1)} = -N_{x1}^{(1)} z_1, \quad u_{11}^{(1)} = 0, \quad w_{11}^{(1)} = 0, \quad M_{y2}^{(2)} = 0, \quad N_{x2}^{(2)} = 0, \quad w_{21}^{(2)} = 0. \quad (1)$$

The first expression in (1) takes into account that the displacement of the left support hinge relative to the end stiffness center will cause the appearance of an initial bending moment.

Substituting (1) into (10) [14], we obtain a system of equations for determining the unknown initial and final parameters

$$\begin{aligned} 0 &= N_{x1}^{(1)} - F_x; \quad Q_{z2}^{(2)} = Q_{z1}^{(1)} + F_z; \quad 0 = lQ_{z1}^{(1)} - N_{x1}^{(1)} z_1 + l_2 F_z + M; \\ u_{21}^{(2)} &= \frac{l}{bB_0} N_{x1}^{(1)} + \frac{z_1 l^2}{2bB_2} Q_{z1}^{(1)} - \frac{z_1 l}{bB_2} N_{x1}^{(1)} z_1 - \frac{l_2 F_x}{bB_0} + \frac{z_1 l_2^2 F_z}{2bB_2} + \frac{z_1 l_2 M}{bB_2}; \\ u_{22}^{(2)} &= \frac{l}{bB_0} N_{x1}^{(1)} + \frac{z_2 l^2}{2bB_2} Q_{z1}^{(1)} - \frac{z_2 l}{bB_2} N_{x1}^{(1)} z_1 + u_{12}^{(1)} - \frac{l_2 F_x}{bB_0} + \frac{z_2 l_2^2 F_z}{2bB_2} + \frac{z_2 l_2 M}{bB_2}; \\ 0 &= -\frac{hl^3 + 6D_2 l}{6hbB_2} Q_{z1}^{(1)} + \frac{l^2}{2bB_2} N_{x1}^{(1)} z_1 - \frac{l}{h} u_{12}^{(1)} - \frac{hl_2^3 + 6D_2 l_2}{6hbB_2} F_z - \frac{l_2^2 M}{2bB_2}. \end{aligned} \quad (2)$$

Having solved (2) in relation to the unknown static and kinematic parameters, we have

$$\begin{aligned} N_{x1}^{(1)} &= F_x, \quad Q_{z1}^{(1)} = \frac{F_x z_1 - l_2 F_z - M}{l}, \quad Q_{z2}^{(2)} = \frac{F_x z_1 + l_1 F_z - M}{l}, \\ u_{21}^{(2)} &= \left(\frac{l_1}{B_0} - \frac{z_1^2 l}{2B_2} \right) \frac{F_x}{b} - \frac{z_1 l_1 l_2 F_z}{2bB_2} + \frac{z_1 (l_2 - l_1) M}{2bB_2}, \\ u_{22}^{(2)} &= \left(\frac{l_1}{B_0} + z_1 \frac{(3z_2 + h)l^2 - 3D_2}{3lB_2} \right) \frac{F_x}{b} - l_1 l_2 \frac{z_2 (l_1 + l) + z_1 (l + l_2)}{6lB_2} \frac{F_z}{b} + \end{aligned} \quad (3)$$

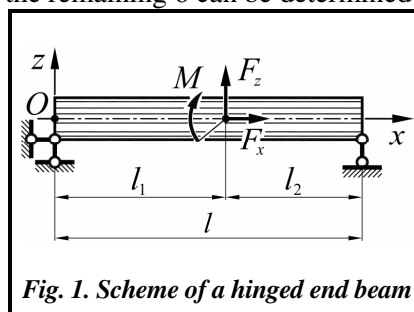


Fig. 1. Scheme of a hinged end beam

$$+ \frac{z_1(3l_2^2 - l^2) - z_2(3l_1^2 - l^2) + 6D_2}{6blB_2} M,$$

$$u_{12}^{(1)} = \frac{z_1(hl^2 - 3D_2)}{3lB_2} \frac{F_x}{b} + \frac{hl_1l_2(l+l_2)F_z}{6blB_2} + \frac{h(l^2 - 3l_2^2) + 6D_2}{6lB_2} \frac{M}{b}.$$

The initial parameters for the second design segment can be determined by substituting (1) and (3) into (11) [14].

It should be noted that in this case the problem is statically determinate, and the static parameters can be determined from the equilibrium conditions of the beam. This allows us to perform an indirect verification of the correctness of the transformations executed.

By substituting the obtained initial parameters into relations (2)–(4) [14], we can obtain expressions for determining all the SSS components on the design segments of the beam under consideration.

For example, determine the deflection of the bottom fiber in the cross-section of the load. Substituting (1) and (3) into the last relation (9) [14], we get

$$w_{21}^{(1)} = \frac{l_1l_2}{3blB_2} \left(-\frac{z_1(l+l_2)}{2} F_x + \left(\frac{3D_2}{h} - l_1l_2 \right) F_z + (l_2 - l_1)M \right). \quad (4)$$

In the case of a homogeneous orthotropic beam with a rectangular cross-section, expression (4) takes the following form:

$$w_{21}^{(1)} = -\frac{l_1l_2(l+l_2)}{lbh^2E_x} F_x + \frac{l_1l_2l}{bh^3E_x} \left(\frac{4l_1l_2}{l^2} + \left(\frac{E_x}{G_{xz}} - \nu_{xz} \right) \frac{h^2}{l^2} \right) F_z - \frac{4l_1l_2(l_2 - l_1)}{lbh^3E_x} M. \quad (5)$$

When the beam is under the action of only the normal component $F_z = -F$ in the middle section ($l_1 = l_2 = l/2$), on the basis of (5), we get the relation

$$w_{21}^{(1)} = \frac{Fl^3}{48bB_2} \left(1 - \frac{12D_2}{hl^2} \right). \quad (6)$$

Equality (6) is similar to the well-known expression for the deflection of an isotropic beam, but in contrast, it contains the component $12D_2/(hl^2)$ that determines the amenability of materials to transverse shear and compression deformations.

For a homogeneous orthotropic beam with a rectangular cross-section, expression (6) takes the following form:

$$w_{21}^{(1)} = -\frac{Fl^3}{4E_xbh^3} \left(1 + \frac{E_x - \nu_{xz}G_{xz}}{G_{xz}} \left(\frac{h}{l} \right)^2 \right). \quad (7)$$

Fixed End Beam. Simulate the rigid fixation of the beam left end (Fig. 2) similarly to the fixation of the console in [12, 13], assuming the displacement of the cross-section extreme points to be zero

$$u_{12}^{(1)} = 0, \quad u_{11}^{(1)} = 0, \quad w_{11}^{(1)} = 0. \quad (8)$$

In the movable fixation of the beam right end, the longitudinal displacements are not equal to zero, but their values in the extreme lower and upper fibers are equal. Then, together with the condition of the absence of longitudinal force and transverse displacements, write such values for the final parameters:

$$N_{x2}^{(2)} = 0, \quad u_{12}^{(2)} = u_{22}^{(2)}, \quad w_{21}^{(2)} = 0. \quad (9)$$

Taking into account (8) and (9), the determining system of equations (10) [14] will take the form

$$0 = N_{x1}^{(1)} - F_x, \quad Q_{z2}^{(2)} = Q_{z1}^{(1)} + F_z, \quad M_{y2}^{(2)} = lQ_{z1}^{(1)} + M_{y1}^{(1)} + l_2F_z + M,$$

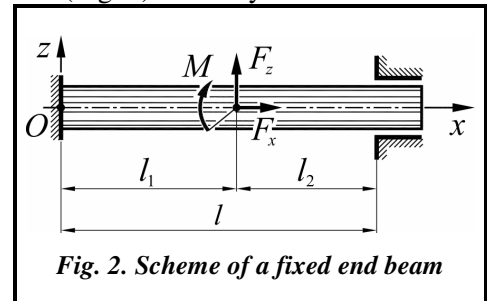


Fig. 2. Scheme of a fixed end beam

$$\begin{aligned}
 u_{22}^{(2)} &= \frac{l}{bB_0} N_{x1}^{(1)} + \frac{z_1 l^2}{2bB_2} Q_{z1}^{(1)} + \frac{z_1 l}{bB_2} M_{y1}^{(1)} - \frac{l_2 F_x}{bB_0} + \frac{z_1 l_2^2 F_z}{2bB_2} + \frac{z_1 l_2 M}{bB_2}, \\
 u_{22}^{(2)} &= \frac{l}{bB_0} N_{x1}^{(1)} + \frac{z_2 l^2}{2bB_2} Q_{z1}^{(1)} + \frac{z_2 l}{bB_2} M_{y1}^{(1)} - \frac{l_2 F_x}{bB_0} + \frac{z_2 l_2^2 F_z}{2bB_2} + \frac{z_2 l_2 M}{bB_2}, \\
 0 &= -\frac{hl^3 + 6D_2 l}{6hbB_2} Q_{z1}^{(1)} - \frac{l^2}{2bB_2} M_{y1}^{(1)} - \frac{hl_2^3 + 6D_2 l_2}{6hbB_2} F_z - \frac{l_2^2 M}{2bB_2}.
 \end{aligned} \tag{10}$$

The solution to system (10) are 6 unknown parameters.

$$\begin{aligned}
 N_{x1}^{(1)} &= F_x, \quad Q_{z1}^{(1)} = -l_2 \frac{(12D_2 - hl_2(l_2 + 3l_1))F_z - 6hl_1 M}{l(12D_2 - hl^2)}, \\
 M_{y1}^{(1)} &= l_2 \frac{(6D_2 l_1 - hl_2 l(2l_2 + l_1))F_z - (12D_2 + hl(2l_1 - l_2))M}{l(12D_2 - hl^2)}, \\
 M_{y2}^{(2)} &= l_1 \frac{(6D_2 - hl_1 l)l_2 F_z + (12D_2 + (3l_2 - l)hl)M}{l(12D_2 - hl^2)}, \\
 Q_{z2}^{(2)} &= l_1 \frac{(12D_2 - hl_1(3l_2 + l_1))F_z + 6hl_2 M}{l(12D_2 - hl^2)}, \quad u_{22}^{(2)} = \frac{l_1 F_x}{B_0 b}.
 \end{aligned} \tag{11}$$

Similarly to the previous example, we obtain the relation for the deflection of the bottom fiber of the beam in the loaded section. By substituting (8) and (11) into the last relation in (9) [14], upon transformation, we get

$$w_{21}^{(1)} = \frac{(2(l_1 l_2)^2 h^2 + 6(12D_2 - h(l^2 + l_1 l_2))D_2)l_1 l_2 F_z + 3h^2(l_1 - l_2)(l_1 l_2)^2 M}{6B_2 b h l (12D_2 - hl^2)}. \tag{12}$$

For the case when only the normal component $F_z = -F$ in the middle cross-section ($l_1 = l_2 = l/2$) acts on the beam, relation (12) can be reduced to

$$w_{21}^{(1)} = \frac{Fl^3}{192bB_2} \left(1 - \frac{48D_2}{hl^2} \right). \tag{13}$$

As in the previous example, relation (13) is similar to the well-known expression for the isotropic beam deflection and also contains a clarifying component.

For a homogeneous beam with a rectangular cross-section, on the basis of (13), we have

$$w_{21}^{(1)} = -\frac{Fl^3}{16bh^3 E_x} \left(1 + 4 \frac{E_x - \nu_{xz} G_{xz}}{G_{xz}} \left(\frac{h}{l} \right)^2 \right). \tag{14}$$

When comparing (7) and (14), it can be noted that in the case of the rigid fixation of beam ends, with all the parameters being the same, the influence of the material amenability to transverse shear and compression deformations on the deflections will be 4 times higher.

Fixed-Hinged Beam. Consider the case when the beam left end is rigidly fixed, and the right one is fixed with a hinged movable support (Fig. 3).

Such types of beam end fixation will be described by the following values of the initial and final parameters:

$$u_{21}^{(1)} = 0, \quad u_{11}^{(1)} = 0, \quad w_{11}^{(1)} = 0, \quad N_{x2}^{(2)} = 0, \quad M_{y2}^{(2)} = 0, \quad w_{21}^{(2)} = 0. \tag{15}$$

Substituting (15) into system (10) [14] and solving the equations obtained, we determine the unknown parameters

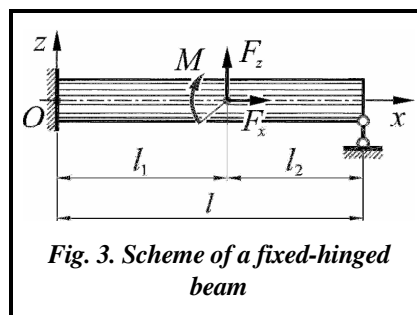


Fig. 3. Scheme of a fixed-hinged beam

$$\begin{aligned}
N_{x1}^{(1)} &= F_x, \quad Q_{z1}^{(1)} = -\frac{(6D_2 + h(l_2^2 - 3l^2))l_2 F_z + 3h(l_2^2 - l^2)M}{2l(3D_2 - hl^2)}, \\
M_{y1}^{(1)} &= -\frac{hl_2(l^2 - l_2^2)F_z + (h(l^2 - 3l_2^2) + 6D_2)M}{2(3D_2 - hl^2)}, \\
Q_{z2}^{(2)} &= \frac{3hl_1(l_2 + l)M + (6D_2 - hl_1(3l_2 + 2l_1))l_1 F_z}{2l(3D_2 - hl^2)}, \\
u_{22}^{(2)} &= \frac{(12D_2 - 4hl^2)l_1 F_x}{4bB_0(3D_2 - hl^2)} + l_1 \frac{(hl_1l - 6D_2)z_2 l_2 F_z - ((3l_2 - l)hl + 12D_2)z_2 M}{4bB_2(3D_2 - hl^2)}, \\
u_{21}^{(2)} &= \frac{(12D_2 - 4hl^2)l_1 F_x}{4bB_0(3D_2 - hl^2)} + l_1 \frac{(hl_1l - 6D_2)z_1 l_2 F_z - ((3l_2 - l)hl + 12D_2)z_1 M}{4bB_2(3D_2 - hl^2)}.
\end{aligned} \tag{16}$$

The relation for the deflection of the bottom fiber of a beam in the loaded cross-section will be obtained in the form

$$w_{21}^{(1)} = \frac{(3l + l_2)h^2 l_1^2 l_2^2 + 12(3D_2 - h(l^2 + l_1 l_2))l_2 D_2}{12B_2 b h l (3D_2 - hl^2)} l_1 F_z + \frac{h(l_1^2 - 2l_2^2) - 6D_2}{4B_2 b l (3D_2 - hl^2)} l_1^2 l_2 M. \tag{17}$$

For the case when only the normal component $F_z = -F$ acts on the beam in the middle cross-section ($l_1 = l_2 = l/2$), (17) can be reduced to

$$w_{21}^{(1)} = \frac{Fl^3}{48bB_2} \left(1 - \frac{12D_2}{hl^2} + \frac{9hl^2}{16(3D_2 - hl^2)} \right). \tag{18}$$

For a homogeneous beam, using (18), we have

$$w_{21}^{(1)} = -\frac{Fl^3}{4bh^3 E_x} \left(1 + \left(\frac{E_x}{G_{xz}} - \nu_{xz} \right) \left(\frac{h}{l} \right)^2 - \frac{9}{16} \left(1 + \frac{1}{4} \left(\frac{E_x}{G_{xz}} - \nu_{xz} \right) \left(\frac{h}{l} \right)^2 \right)^{-1} \right). \tag{19}$$

Similarly, we can obtain solutions to other problems of bending double-support multi-layer beams with a more complex description of different types of beam end fixations, which takes into account, for example, their amenability, draft or inaccuracy of installation.

As an example of the implementation of the relations obtained, we consider the results of their use in determining the SSS components of homogeneous and four-layer beams of the $h \times b = 100 \times 15$ mm rectangular cross-section.

Model Approximation

Homogeneous beam. In this case, we consider carbon-fiber beams ($E_x = 142.8$ GPa, $G_{xz} = 5.49$ GPa, $\nu_{xz} = 0.32$), loaded with the force $F_z = -17500$ N in the middle section ($l_1 = l_2 = l/2$) with different fixation methods.

For the indicated initial data based on relations (7), (14), and (19), the deflection of the bottom fiber of the beam in the loaded section was calculated. The results of the calculation of beams with different lengths are summarized in the table below.

For comparison, the table shows the results of FEM simulation using Plate-type elements, the calculation results using the flat section hypothesis ($G_{xz} = \infty$, $\nu_{xz} = 0$), as well as the results of the calculation using the iteration model of the first approximation [10].

The data in the table show a slight discrepancy between the results of calculation using the obtained relations, FEM, and iteration model, which decreases with increasing the relation l/h . At the same time, the use of the hypothesis of flat sections leads to significant errors in determining the deflections, from 22 to 80%, depending on the type of beam end fixation.

The results of calculating the beam bottom fiber deflection, mm

Beam length	Solution obtained	FEM modeling	Hypothesis of flat cross-sections	Iteration model
Hinged end beam (Fig. 1)				
$l=5h$	-0.5177	-0.5399	-0.2553	-0.5516
$l=10h$	-2.5672	-2.6183	-2.0425	-2.6576
Fixed end beam (Fig. 2)				
$l=5h$	-0.3262	-0.3216	-0.0638	-0.3377
$l=10h$	-1.0354	-1.0757	-0.5106	-1.1033
Fixed-hinged end beam (Fig. 3)				
$l=5h$	-0.4034	-0.4085	-0.1117	-0.3964
$l=10h$	-1.4877	-1.5414	-0.8936	-1.4973

Four-layer beam. It is accepted that the $l = 10h$ four-layer beam has a combined end fixation (Fig. 3) and is loaded with the force $F_z = -17500$ N in the section $x = l_1 = 4h$. The structure and dimensions of the beam cross-section are shown in Fig. 4.

For the materials of the layers, the following values of the elastic characteristics are taken:

- P_1 (aluminium alloy) – $E_x^{[1]} = 70$ GPa, $G_{xz}^{[1]} = 26.9$ GPa, $\nu_{xz}^{[1]} = 0.34$;
- P_2 (wood) – $E_x^{[2]} = 12.1$ GPa, $G_{xz}^{[2]} = 1.21$ GPa, $\nu_{xz}^{[2]} = 0.49$;
- P_3 (fiberglass) – $E_x^{[3]} = 36.8$ GPa, $G_{xz}^{[3]} = 4.5$ GPa, $\nu_{xz}^{[3]} = 0.351$;
- P_4 (black-reinforced plastic) – $E_x^{[3]} = 142.8$ GPa, $G_{xz}^{[3]} = 5.49$ GPa, $\nu_{xz}^{[3]} = 0.32$.

The position of the stiffness center and characteristics of the cross-sectional stiffness are obtained using the relations given in [14]

$$z_{B_1} = 58,41 \text{ mm}, B_2 = -5298,64 \cdot 10^3 \text{ N}\cdot\text{m}, D_2 = -3472,31 \cdot 10^{-6} \text{ m}^3.$$

Using relations (2)–(4), (11) from [14] and relations (15) and (16) obtained above, we have expressions for the SSS components of the calculated beam segments. These expressions were combined into general expressions for the entire beam according to (6) [14].

The stress distribution in the cross-section $x = h$ for a multi-layer beam is shown in Fig. 5, which also shows the distribution of the longitudinal modulus of elasticity. The dashed line shows the stresses obtained using the hypothesis of flat cross-sections ($G_{xz} = \infty, \nu_{xz} = 0$).

The maximum values of the stresses σ_x in the lower and upper layers differ from those obtained in the FEM calculation by 6 and 0.8%, respectively. The use of the hypothesis of flat cross-sections leads to an increase in stress values by 18 and 26%.

This can be explained by an increase in the calculated value of the support reactive moment in the rigid fixation when the hypothesis of flat cross-sections is used. The obtained relations give the value of the bending moment $M_{y1} = 3043$ N·m, and the application of the hypothesis of flat cross-sections leads to its increase by 10.4% to $M_{y1} = 3360$ N·m.

Separate displacement distribu-

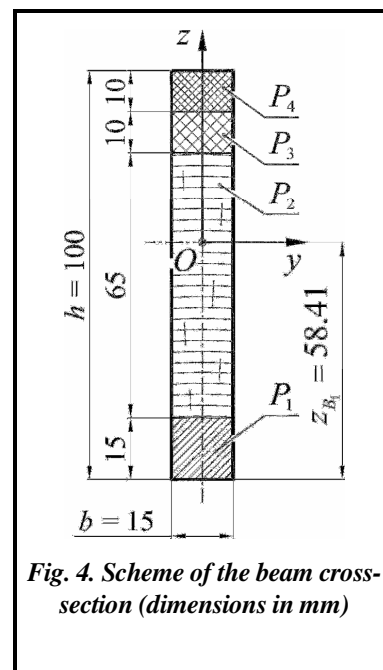


Fig. 4. Scheme of the beam cross-section (dimensions in mm)

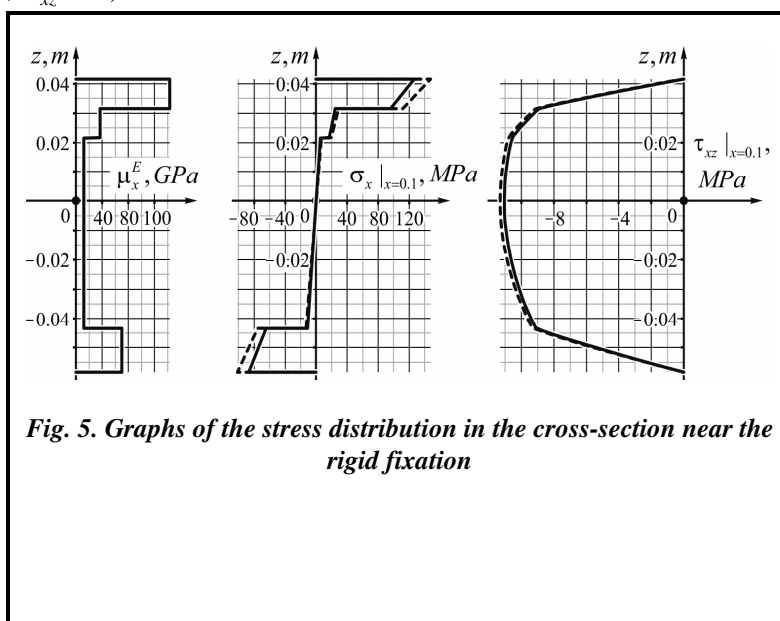


Fig. 5. Graphs of the stress distribution in the cross-section near the rigid fixation

tions are shown in Fig. 6, where the dashed line shows the displacements obtained using the hypothesis of flat cross-sections.

The graph for the longitudinal displacements (Fig. 6, a) shows the curvature of the cross-sections under the action of the transverse force, which cannot be predicted using the hypothesis of flat cross-sections. The comparison of the obtained value of the longitudinal displacements in the extreme fibers of the beam with the FEM

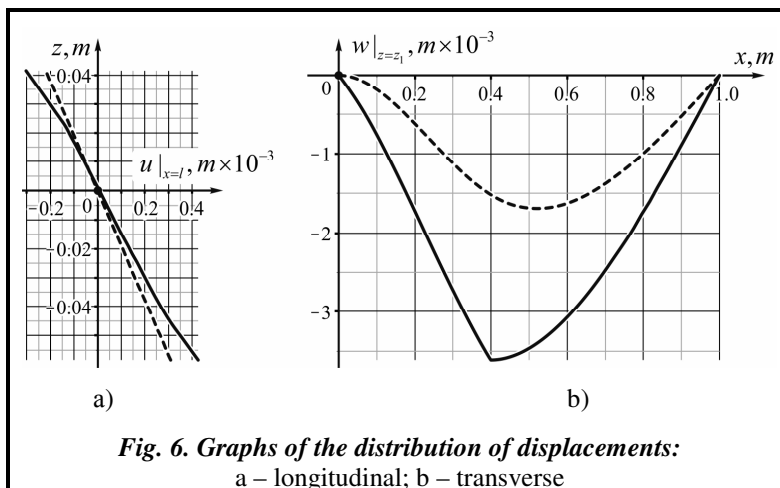


Fig. 6. Graphs of the distribution of displacements:
a – longitudinal; b – transverse

simulation results shows a small difference (up to 7%). However, near the rigid fixation and the loaded section, the difference from the results of the FEM calculation increases.

The deflection of the bottom fiber of the beam (Fig. 6, b) in the loaded section according to the obtained relations was 3.61 mm, which is only 1.7% higher than the value obtained by FEM simulation ($w|_{x=l_1, z=z_1} = 3.55$ mm). At the same time, the application of the hypothesis of flat sections leads to a decrease in the deflection by 57%, up to $w|_{x=l_1, z=z_1} = 1.52$ mm.

Using the obtained analytical relations for the displacements, an after-deformation beam shape is constructed, with the displacements increased 40-fold (Fig. 7). For comparison, Fig. 7, b shows the shape of an after-deformation beam constructed based on the relations for the displacements, which are obtained using the hypothesis flat cross-sections.

The fracture of the deformed fibers of the beam in the loaded section in Fig. 7, a and the shift of the maximum deflection of the beam result from both the simplification of the kinematic conditions for the joint deformation of the design segments and rigid fixation. It should be noted

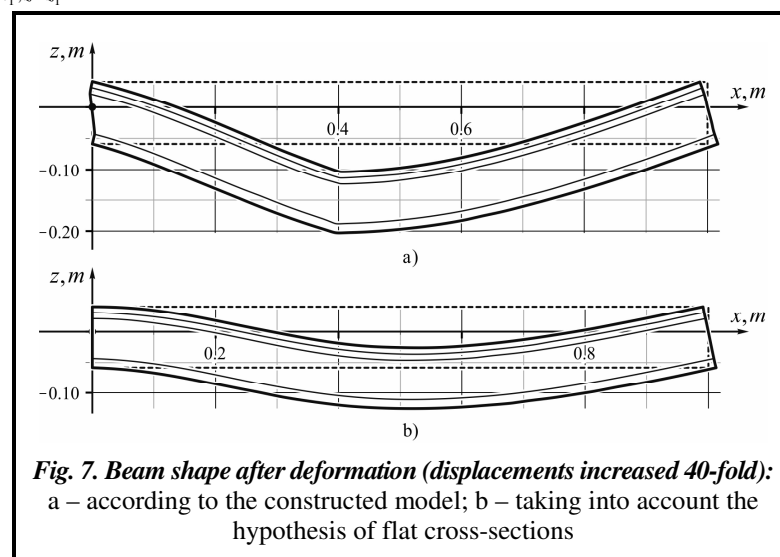


Fig. 7. Beam shape after deformation (displacements increased 40-fold):
a – according to the constructed model; b – taking into account the hypothesis of flat cross-sections

that such a distribution of displacements, in general, turns out to be much closer to the results of the calculation by FEM and the iterative model than that obtained using the hypothesis of flat cross-sections (Fig. 7, b). The picture of displacement distribution can be clarified by improving the relevant kinematic conditions. However, this will obviously lead to a complication of the final relations.

Conclusions

Thus, on the basis of the constructed simple bending model of double-support multi-layer beams under a concentrated load, particular solutions are obtained for the main SSS of beams with different combinations of fixation of their extreme sections.

The obtained relations were approved when we solved the test problems of bending homogeneous orthotropic and four-layer beams with different types of beam end fixation. The comparison of the obtained results for individual SSS components with the results of FEM simulation and calculation by an iteration model shows good convergence with the exception of the zones near the loaded and fixed cross-sections. At the same time, the use of the hypothesis of flat cross-sections leads to significant errors in the determination of displacements, and for statically indefinable problems, also internal force factors and stresses.

The demonstrated approaches to solving bending problems can be used without difficulty in the process of constructing solutions to more complex applied problems of bending multilayer beams with various combinations of loading and fixation.

References

1. Altenbakh, K. H. (1998). *Osnovnyye napravleniya teorii mnogosloynnykh konsyruksiy. Obzor* [Major directions of the theory of multilayer thin-walled structures. Survey]. *Mekhanika kompozitnykh materialov – Mechanics of composite materials*, no. 3, pp. 333–348 (in Russian).
2. Ambartsumyan, S. A. (1987). *Teoriya anizotropnykh plastin* [Theory of anisotropic plates]. Moscow: Nauka, 360 p. (in Russian).
3. Bolotin, V. V. & Novichkov, Yu. N. (1980). *Mekhanika mnogosloynnykh konstruksii* [Mechanics of multilayer structures]. Moscow: Mashinostroyeniye, 374 p. (in Russian).
4. Vasilyev, V. V. (1988). *Mekhanika konstruksiy iz kompozitsionnykh materialov* [Mechanics of structures made of composite materials]. Moscow: Mashinostroyeniye, 272 p. (in Russian).
5. Grigolyuk, E. I. & Selezov, I. T. (1972). *Neklassicheskaya teoriya kolebaniy sterzhney, plastin i obolochek. Itogi nauki i tekhniki* [Non-classical theory of oscillations of rods, plates and shells. Results of science and technology (Vol. 5)]. Moscow: Nauka, 271 p. (in Russian).
6. Guz, A. N., Grigorenko, Ya. M., Vanin, G. A., & Babich I. Yu. (1983). *Mekhanika elementov konstruksiy: V 3 t, T. 2: Mekhanika kompozitnykh materialov i elementov konstruksiy* [Mechanics of structural elements (Vol. 1–3): Mechanics of composite materials and structural elements (Vol. 2)]. Kiyev: Naukova dumka, 484 p. (in Russian).
7. Malmeyster, A. K., Tamuzh, V. P., & Teters, G. A. (1980). *Soprotivleniye polimernykh i kompozitnykh materialov* [Resistance of polymeric and composite materials]. Riga: Zinatne, 572 p. (in Russian).
8. Rasskazov, A. O., Sokolovskaya, I. I., & Shulga, N. A. (1987). *Teoriya i raschet sloistykh ortotropnykh plastin i obolochek* [Theory and calculation of layered orthotropic plates and shells]. Kiyev: Vyscha shkola, 200 p. (in Russian).
9. Piskunov, V. G. (2003). *Iteratsionnaya analiticheskaya teoriya v mekhanike sloistykh kompozitnykh system* [Iterative analytical theory in mechanics of layered composite systems]. *Mekhanika kompozit. materialov – Mechanics of Composite Materials*, vol. 39, no. 1, pp. 2–24 (in Russian). <https://doi.org/10.1023/A:1022979003150>
10. Horyk, O. V., Piskunov, V. H., & Cheredniko, V. M. (2008). *Mekhanika deformuvannia kompozytnykh brusiv* [Mechanics of deformation of composite beams]. Poltava; Kyiv: ASMI, 402 p. (in Ukrainian).
11. Goryk, A. V. (2001). Modeling transverse compression of cylindrical bodies in bending. *Intern. Appl. Mech.*, vol. 37, iss. 9, pp. 1210–1221. <https://doi.org/10.1023/A:1013294701860>
12. Goryk, A. V. & Koval'chuk, S. B. (2018). Elasticity theory solution of the problem on plane bending of a narrow layered cantilever bar by loads at its end. *Mech. Composite Materials*, vol. 54, iss. 2, pp. 179–190.
13. Goryk, A. V. & Koval'chuk, S. B. (2018). Solution of a transverse plane bending problem of a laminated cantilever beam under the action of a normal uniform load. *Strength of Materials*, vol. 50, iss. 3, pp. 406–418. <https://doi.org/10.1007/s11223-018-9984-7>
14. Kovalchuk, S. B. & Gorik, A. V. (2018). Major stress-strain state of double support multilayer beams under concentrated load. Part 1. Model construction. *J. Mech. Eng.*, vol. 21, no. 4, pp. 30–36.

Received 26 September 2018

Основний напружено-деформований стан двохопорних багатошарових балок під дією зосередженого навантаження. Частина 2. Реалізація моделі та результати розрахунку

Ковальчук С. Б., Горик О. В.

Полтавська державна аграрна академія, 36003, Україна, м. Полтава, вул. Сковороди, 1/3

Розвиток технологій композитів сприяє їх широкому впровадженню в практику проектування сучасних конструкцій різного призначення. Достовірне прогнозування напружено-деформованого стану композитних елементів є однією з умов створення надійних конструкцій з оптимальними параметрами. Аналітичні теорії визначення напружено-деформованого стану багатошарових стрижнів (брусів, балок) значно поступаються у розвитку теоріям для композитних плит і оболонок, хоча стрижневі елементи конструкцій є найпоширенішими. Метою даної роботи є побудова аналітичної моделі вигину двохопорних багатошарових балок під дією зосередженого навантаження на основі отриманого раніше розв'язку теорії пружності для багатошарової консолі. У другій частині статті наведені приклади реалізації моделі згину двохопорних багатошарових балок під дією зосередженого навантаження, побудованої у першій частині статті. Із використанням моделі отримано розв'язку задач згину багато-

шарових балок з різними способами закріплення їх крайніх перерізів. Отримані співвідношення апробовані на тестових задачах визначення прогинів однорідних композитних двохопорних балок з різними комбінаціями закріплення, а також під час визначення напружень і переміщень чотиришарової балки з жорстким і шарнірним закріпленням торців. Отримані результати мають незначну розбіжність з результатами моделювання методом скінченних елементів і розрахунку по ітераційній моделі згину композитних брусів, навіть для відносно коротких балок. Крім того, показано, що нехтування зсувною піддатливістю матеріалів шарів призводить до великих похибок під час визначення прогинів, а у разі статично невизначених балок – також реактивних зусиль і напружень. Застосований під час побудови моделі підхід можна розширити на випадок балок з будь-якою кількістю зосереджених сил і проміжних опор та для розрахунку багатошарових балок з різними жорсткостями розрахункових ділянок.

Ключові слова: багатошарова балка, ортотропний шар, зосереджене навантаження, напруження, переміщення.

Література

- 1.Альтенбах Х. Основные направления теории многослойных тонкостенных конструкций. Обзор. *Механика композит. материалов.* 1998. № 3. С. 333–348.
- 2.Амбарцумян С. А. Теория анизотропных пластин. М.: Наука, 1987. 360 с.
- 3.Болотин В.В., Новичков Ю. Н. Механика многослойных конструкций. М.: Машиностроение, 1980. 374 с.
- 4.Васильев В. В. Механика конструкций из композиционных материалов. М.: Машиностроение, 1988. 272 с.
- 5.Григолюк Э. И., Селезов И. Т. Неклассическая теория колебаний стержней, пластин и оболочек. *Итоги науки и техники.* М.: Наука, 1972. Т. 5. 271 с.
- 6.Гузь А. Н., Григоренко Я. М., Ванин Г. А., Бабич И. Ю. Механика элементов конструкций: В 3 т. Т. 2: Механика композитных материалов и элементов конструкций. Киев: Наук. думка, 1983. 484 с.
- 7.Малмейстер А. К., Тамуж В. П., Тетерс Г. А. Сопrotивление полимерных и композитных материалов. Рига: Зинатне, 1980. 572 с.
- 8.Рассказов А. О., Соколовская И. И., Шульга Н. А. Теория и расчет слоистых ортотропных пластин и оболочек. Киев: Вища шк., 1987. 200 с.
- 9.Пискунов В. Г. Итерационная аналитическая теория в механике слоистых композитных систем. *Механика композит. материалов.* 2003. Т. 39. № 1. С. 2–24. <https://doi.org/10.1023/A:1022979003150>
10. Горик О. В., Пискунов В. Г., Чередников В. М. Механіка деформування композитних брусів. Полтава; Київ: АСМІ, 2008. 402 с.
11. Goryk A. V. Modeling transverse compression of cylindrical bodies in bending. *Intern. Appl. Mech.* 2001. Vol. 37. Iss. 9. P. 1210–1221. <https://doi.org/10.1023/A:1013294701860>
12. Goryk A. V., Koval'chuk S. B. Elasticity theory solution of the problem on plane bending of a narrow layered cantilever bar by loads at its end. *Mech. Composite Materials.* 2018. Vol. 54. Iss. 2. P. 179–190.
13. Goryk A. V. Koval'chuk S.B. Solution of a transverse plane bending problem of a laminated cantilever beam under the action of a normal uniform load. *Strength of Materials.* 2018. Vol. 50. Iss. 3. P. 406–418. <https://doi.org/10.1007/s11223-018-9984-7>
14. Kovalchuk S. B., Gorik A. V. Major stress-strain state of double support multilayer beams under concentrated load. Part 1. Model construction. *J. Mech. Eng.* 2018. Vol. 21. No. 4. P. 30–36.